Vibration Suppression of A Middle-Point Current-Injection Type Bearingless Motor at 50000r/min

Yusuke Uemura, Takayuki Nakahata, Akira Chiba*

Tokyo Institute of Technology, 2-12-1 Ookayama Meguro, Tokyo, Japan

***Abstract*— With the developments of power electronics technology and increments of rotational speed of motors, a critical speed is one of the problems. Vibration of rotational shaft has been reported to be suppressed by magnetic force of bearingless motors. In general bearingless motors, motor windings and suspension windings are separately enclosed in the stator slot. For only vibration suppression at a critical speed, however, suspension windings are not used except the critical speed. In this paper, vibration suppression of a rotor shaft by a middle-point current-injection type bearingless motor at 50000 r/min is presented. This motor can generate the torque and the magnetic force by only one set of three-phase windings. The test results of the vibration suppression are presented.**

I. INTRODUCTION

In recent years, the developments of power electronics technology and the appearances of strong permanent magnets and iron materials with low iron losses make possible to increase a motor rotational speed. High speed motors and generators are applied to turbines, superchargers and compressors. The critical speed is one of the serious problems in the high speed motor. The vibration of a rotor shaft at the critical speed is caused by resonance of the shaft natural frequency. In the worst case, the rotor shaft may be broken. Thus, various solutions for the vibration suppression have been studied.

To solve the problems, bearingless motors have been proposed. The bearingless motors combine a magnetic bearing and a motor function [1-14]. The advantages are low cost and small size compared with magnetic bearing motors. The Finland group and the authors reported the vibration suppression and operation over the critical speed with a bearingless motor [15-16]. In these bearingless motors, two sets of windings are installed in the stator slots. One set is the motor winding for the torque generation, and another set is the suspension winding for the radial magnetic force generation. However, in the vibration suppression, the suspension winding is not excited except the critical speed. Furthermore, the requirement of the additional suspension conductors causes torque reduction, or increased stator dimensions.

In the literatures, there are some bearingless motors which generate the torque and the magnetic force by only one set of three-phase winding. The bridge configured winding type bearingless motor [17] is one of the novel structures. The winding coils are separated and radial force currents are injected in the bridge circuit structure. This structure needs three units of a single-phase inverter for x- and y-axis force generation. Therefore, the cost of the bearingless motor driver is high. A simple homopolar winding structure for an induction motor bearingless motor has been proposed [18]. This winding structure is simple, however, an additional homopolar winding is necessary in addition to a three-phase winding. The authors have proposed a middle-point current-injection type bearingless motor [19]. The proposed bearingless motor has simple structure and does not require an additional winding because vibration suppression inverter is connected to the middle-points in the motor winding. In addition, the motor driver and a controller do not need modification. Suppression vibration of rotor shaft and operation over the critical speed (7200 r/min) was reported. The principle of this bearingless motor applied at a rotational speed up to 10000r/min. In [19-20], a controller with a DSP is applied, however, the calculation was not fast enough for the target speed of 100,000r/min.

In this paper, the principle of a middle-point current-injection type bearingless motor is applied to a high-speed prototype machine. The controllers are based on analog circuits and a FPGA as well as a microcomputer. The vibration suppression is confirmed at a critical speed of 50000r/min.

II. WINDING STRUCTURE

Fig. 1 shows an example of the stator winding structure for two-pole SPM rotor in the proposed middle-point current-injection type bearingless motor. Fig. 2 shows the connection between the coils and the three-phase inverters. In the middle-point current-injection type bearingless motor, only one set of three-phase winding is installed in the stator slots. The *U*, *V* and *W* phase windings are installed by every 120 degrees so that 2-pole three-phase windings are built. The *U*, *V* and *W* phase motor currents i_{MU}, i_{MV} and i_{MW} generate 2-pole magnetic flux in the air gap to generate torque. On the other hands, the suspension currents i_{SU}, i_{SW} and i_{SV} are injected to the middle-points of each phase in order to generate 4-pole magnetic flux in the air gap to generate radial magnetic force. Consequently, both the motor and suspension currents are provided in the windings of U_2, V_2 and W_2.

*corresponding author

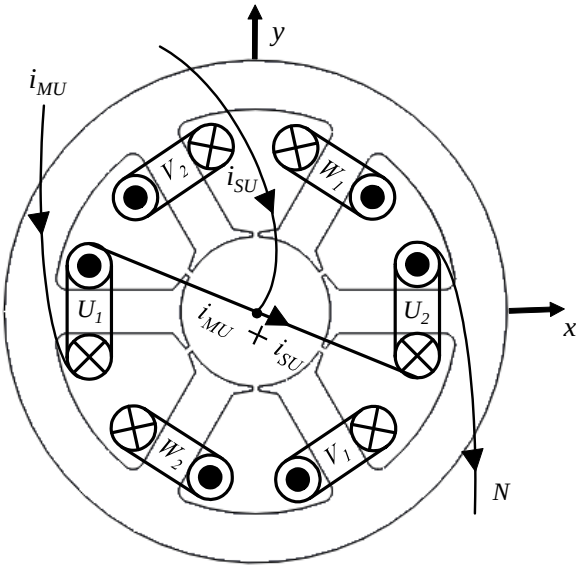

Fig. 1. Stator structure of the proposed middle-point current-injection type bearingless motor.

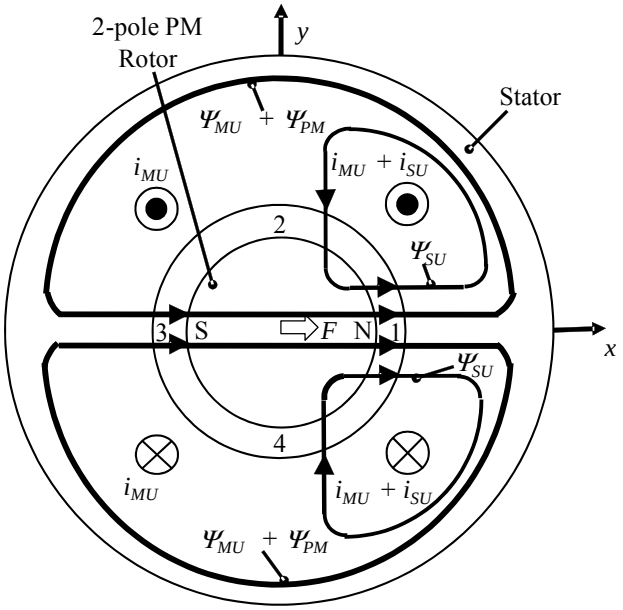

Fig. 3. Principle of radial force generation with the proposed middle-point current-injection type bearingless motor.

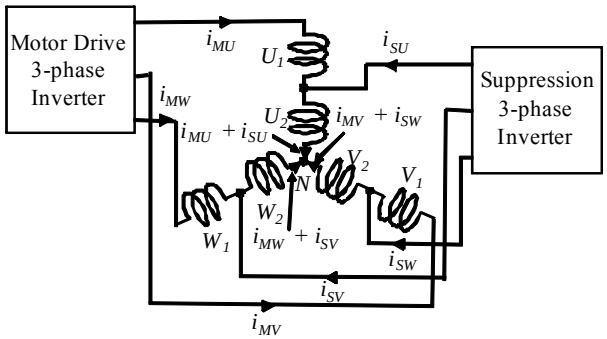

Fig. 2. Connection of windings and inverters in the proposed middle-point current-injection type bearingless motor.

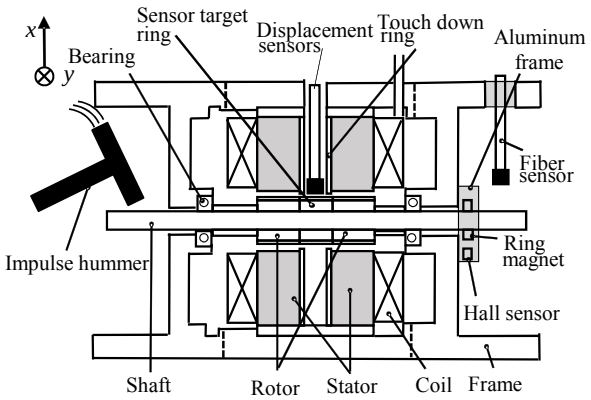

Fig. 4. Structure of the high speed test machine.

III. Principle of Radial Magnetic Force Generation

Fig. 3 shows principle of radial force generation with the proposed middle-point current-injection type bearingless motor. Only U-phase winding is illustrated. In the left-side conductors U_1, only the motor current i_{MU} is provided. On the contrary, in the right-side the suspension current i_{SU} is added to the motor current i_{MU}. As the result, the 2-pole flux $\Psi_{MU} + \Psi_{PM}$ is generated by the 2-pole motor current and the rotor PM. In addition, 4-pole flux Ψ_{SU} is generated in the right half side by the suspension current. The $\Psi_{MU} + \Psi_{PM}$ and Ψ_{SU} are the same direction in the air gap 1, and thus, air gap magnetic flux density is increased. Therefore, the radial suspension force is generated in the positive *x*-direction because the flux density in the air gap 1 is high compared with that in the air gap 3. When the i_{SU} is negative, the radial suspension force is generated in the negative *x*-direction because the flux density in the air gap 1 is low compared with that in the air gap 3.

IV. Experimental System

A. Prototype Machine Structure

Fig. 4 shows the cross-sectional view of a test machine. The both ends of the rotational shaft is suspended by the ball bearings. The stator consists of two iron cores with only two coil ends. Three displacement sensors are installed between the stator cores. A touch-down ring is installed in the stator to protect the eddy current type sensors. The touch-down gap length between the touch-down ring and the sensor target is 500 μm. Two hall sensors are installed to aluminum frame

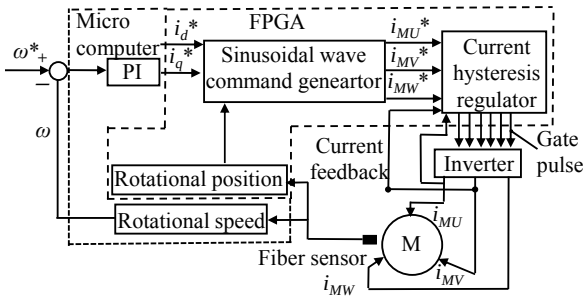

Fig.5. Block diagram of the motor drive system.

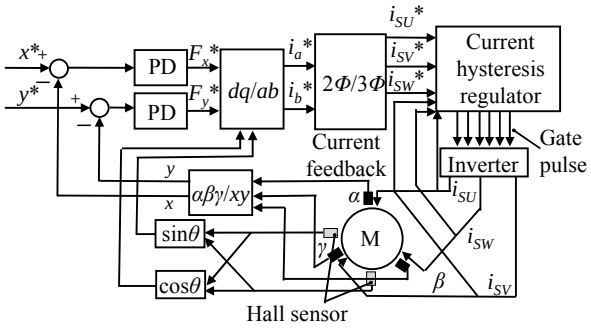

Fig.6. Block diagram of the vibration suppression system.

fixed to the right end. A fiber sensor for motor speed regulation is also installed, however, this is not necessary.

B. Motor Drive And Vibration Suppression System

Fig. 5 shows a block diagram of the motor drive system. The PI regulator and rotational speed calculation are realized in a microcomputer. A sinusoidal wave command generation, a current hysteresis regulator and a rotational position calculation are realized in the FPGA. The rotational speed signal ω is compared with the speed reference ω^*. The error signal is amplified by a proportional-integral (PI) regulator, and torque current reference i^*_q is generated. Based on the rotor rotational angular position, the current references i^*_q and i^*_d are transformed into sinusoidal current references i^*_{MU}, i^*_{MV} and i^*_{MW}. In the current hysteresis regulator, the current references i^*_{MU}, i^*_{MV} and i^*_{MW} are compared with the detected currents. Gate pulse signals are generated in the current hysteresis regulator. The PWM signals are given to the motor inverter, and the three-phase motor currents are regulated.

Fig. 6 shows the block diagram of the vibration suppression system. Analog circuits are adapted in the vibration suppression regulation system. Three displacement sensors are installed every 120 degrees in the stator. The detected signals are transformed into two perpendicular displacements x and y. The position references x^* and y^* are zero. The error signals between the references and the detected feedback signals are input in the proportional-

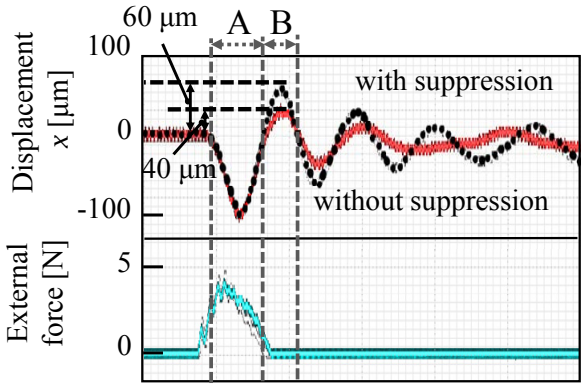

Fig.7. Waveforms of shaft vibration with and without suppression regulation.

derivative regulators, and then, radial magnetic force references F^*_x and F^*_y are generated. The radial magnetic force references are transformed into three-phase current references. The three-phase current references i^*_{SU}, i^*_{SV} and i^*_{SW} are given to the current hysteresis regulator. Thus, suspension currents are injected at the middle point in the motor main windings.

V. EXPERIMENTAL RESULTS

Fig. 7 shows waveforms of the shaft vibration and external force with and without suppression feedback regulation in static condition. The vibration is given by an impulse hummer, which provides force at the end of shaft. The impulse hummer has output terminals to observe the applied external force. The vibration is measured by displacement sensors. In this experiment, the external force is about 5 N. The effect of vibration suppression regulation does not appear in the section A because the impulse hammer is touching to the rotor shaft. The maximum displacement without the suppression regulation in the section B is 60 μm. On the other hands, the maximum displacement with the suppression regulation in the section B is 40 μm. The vibration in the section B is decrease by 33 %.

Figs. 8 (a) and (b) show the waveforms of the vibration with and without the suppression regulation, respectively, at the rotational speed of 50000 r/min. The vibration peak to peak amplitudes without suppression regulation are 400 μm in the x- and y-axes. When suppression regulation is applied, the vibration peak to peak amplitudes are reduced to 320 μm in the x- and y-axes. Thus, the vibration is decreased by 20 %, respectively. The effectiveness is limited, however, better mechanical balancing is needed for future experiments.

VI. CONCLUSION

In this paper, development and experimental results of vibration suppression of 50000r/min test motor have been described. The vibration is suppressed by the current injection at the middle points of motor windings. The injected current make the magnetic field unbalanced, thus, radial force can be generated in two perpendicular axes. By detecting the rotor

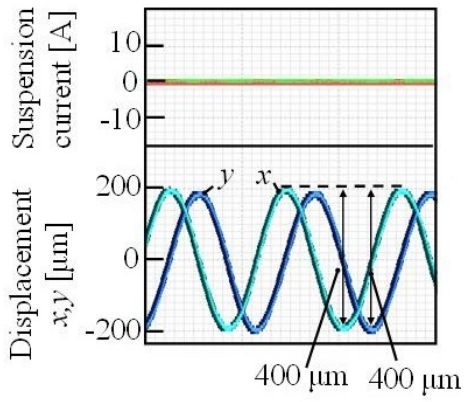

(a)Without suppression.

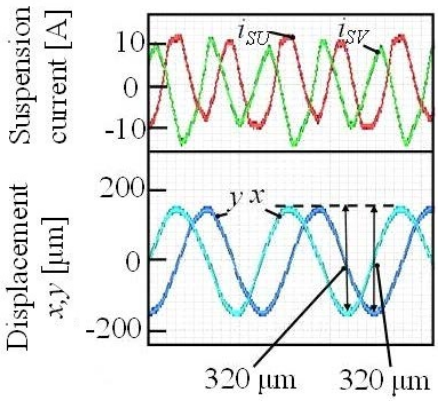

(b)With suppression.

Fig.8. Waveforms of shaft vibration with and without suppression regulation at rotational speed of 50000 r/min.

vibration, feedback controllers have been developed. The effectiveness has been verified in principle.

REFERENCES

[1] Ribeiro, R.L.A.; Castro, F.E.F.; Salazar, A.O.; Maitelli, A.L.; , "A Suitable Current Control Strategy for Split-Phase Bearingless Three-Phase Induction Machine," Power Electronics Specialists Conference, 2005. PESC '05. IEEE 36th , vol., no., pp.701-706, 16-16 June 2005

[2] Gruber, W.; Amrhein, W.; Haslmayr, M.; , "Bearingless Segment Motor With Five Stator Elements—Design and Optimization," Industry Applications, IEEE Transactions on , vol.45, no.4, pp.1301-1308, July-aug. 2009

[3] Gruber, W.; Nussbaumer, T.; Grabner, H.; Amrhein, W.; , "Wide Air Gap and Large-Scale Bearingless Segment Motor With Six Stator Elements," Magnetics, IEEE Transactions on , vol.46, no.6, pp.2438-2441, June 2010

[4] J. Asama, R. Kawata, T. Tamura, T. Oiwa, and A. Chiba, "Reduction of Force Interference and Performance Improvement of a Consequent-Pole Bearingless Motor", Precision Engineering, Vol.36, Issue 1, pp. 10-18, January 2012.

[5] Akira Chiba, Tadashi Fukao, Osamu Ichikawa, Masahide Oshima, Masatsugu Takemoto and David G. Dorrell, "Magnetic Bearings and Bearingless Drives", Newnes Elsevier, ISBN 0 7506 5727 8, 2005

[6] Akira Chiba, Tazumi Deido, Tadashi Fukao and M.A.Rahman, "An Analysis of Bearingless ac Motors", IEEE Transactions on Energy Conversion, vol.9, no.1, pp.61-68, 1994

[7] J. Asama, Y. Hamasaki, T. Oiwa, and A. Chiba, "A Novel Concept of a Single-Drive Bearingless Motor", Proceedings of the IEEE International Electric Machines and Drives Conference (IEMDC) 2011, Niagara Falls, 15 –18 May, 2011.

[8] S. Silber, et al., "Design aspects of bearingless slice motors", IEEE/ASME Trans. Mechatronics, vol. 10, no. 6, pp. 611 – 617, Dec. 2005.

[9] Z. Ren and L. S. Stephens : "Closed-Loop Performance of a Six Degree-of-Freedom Precision Magnetic Actuator", IEEE/ASME Trans. Mechatronics, Vol.10, No.6 pp-666-674 (2005)

[10] H. Kanebako, Y. Okada, "New design of hybrid-type self-bearing motor for small, high-speed spindle," IEEE Trans. Mechatronics, vol.8, no.1, pp. 111-119, Mar. 2003.

[11] J. Amemiya, A. Chiba, D. G. Dorrell and T. Fukao, "Basic Characteristics of a Consequent-Pole-Type Bearingless Motor," IEEE Trans. Magn., vol. 41, no. 1, pp.82-89, Jan. 2005.

[12] T. Schneeberger, T. Nussbaumer and J. W. Kolar, "Magnetically Levitated Homopolar Hollow-Shaft Motor," IEEE/ASME Trans. Mechatronics, vol. 15, no. 1, pp. 97 – 107, Feb. 2010.

[13] J. Asama, T. Asami, T. Imakawa, A. Chiba, A. Nakajima and M. A. Rahman, "Effects of Permanent-Magnet Passive Magnetic Bearing on a Two-Axis Actively Regulated Low-Speed Bearingless Motor," IEEE Trans. Energy Conversion, vol. 26, no. 1, pp. 46 – 54, Mar. 2011.

[14] N. Watanabe, H. Sugimoto, A. Chiba, T. Fukao, "Basic Characteristic of the Multi-Consequent-pole Bearingless Motor," in Proc. PCC Nagoya, pp.1565-1570, 2-5 Apr. 2007.

[15] Antti Laiho, Anssi Sinervo, Juha Orivuori, Kari Tammi, Antero Arkkio and Kai Zenger : "Attenuation of harmonic rotor vibration in a cage rotor induction machine by a self- bearing force actuator", *IEEE Trans. Magnetics 2009*, vol.45, No.12, pp.1-2 (2009)

[16] Akira Chiba, Tadashi Fukao, M. Azizur Rahman : "Vibration Suppression of a Flexible Shaft With a Simplified Bearingless Induction Motor Drive", *IEEE Trans. Industry Applications*, vol.44, Issue.4, pp.745-752 (2008).

[17] W. K. S. Khoo, Kalita K, Garvey S.D. : "Practical Implementation of the Bridge Configured Winding for Producing Controllable Transverse Forces in Electrical Machines", *IEEE Trans. Industry Magnetics*, vol.47, No.6, pp.1712-1718 (2011)

[18] A. Sinervo, T. Jokela, A. Arkkio,"Controlling Rotor Vibrations of a Two-Pole Induction Machine With Unipolar Actuator", IEEE Transactions on Magnetics Vol.48, no.7, 2012, pp.2205 - 2210

[19] A. Chiba, K.Sotome, Y. Iiyama, M. A. Rahman : "A Novel Middle-Point-Current-Injection-Type Bearingless PM Synchronous Motor for Vibration Suppression", *IEEE Trans. Industry Applications*, vol.47, Issue.4, pp.1700-1706 (2008)

[20] Ryohei Oishi, Satoshi Horima, Hiroya Sugimoto and Akira Chiba, "A Novel Parallel Motor Winding Structure for Bearingless Motors", IEEE Transactions on Magnetics, vol.49, no.5, May 2013, pp. 2287-2290